대한영상의학회지

Scoring System to Predict Malignancy for MRI-Detected Lesions in Breast Cancer Patients: Diagnostic Performance and Effect on Second-Look Ultrasonography

유방암 환자의 MRI에서 발견된 병변의 악성 예측을 위한 점수체계: 진단적 능력과 이차 초음파 결정에 미치는 영향

Young Geol Kwon, MD (iD), Ah Young Park, MD* (iD)

Department of Radiology, CHA Bundang Medical Center, CHA University, Seongnam, Korea

*Corresponding author
Ah Young Park, MD
Department of Radiology,
CHA Bundang Medical Center,
CHA University, 59 Yatap-ro,
Bundang-gu,
Seongnam 13496, Korea.

Tel 82-31-780-5000
Fax 82-31-780-5381
E-mail pay526@cha.ac.kr

ORCID iDs
Young Geol Kwon (iD)
https://
orcid.org/0000-0001-8352-8529
Ah Young Park (iD)
https://
orcid.org/0000-0002-4747-9480

Purpose To design a scoring system to predict malignancy of additional MRI-detected lesions in breast cancer patients.

Materials and Methods Eighty-six lesions (64 benign and 22 malignant) detected on preoperative MRI of 68 breast cancer patients were retrospectively included. The clinico-radiologic features were correlated with the histopathologic results using the Student's t-test, Fisher's exact test, and logistic regression analysis. The scoring system was designed based on the significant predictive features of malignancy, and its diagnostic performance was compared with that of the Breast Imaging-Reporting and Data System (BI-RADS) category.

Results Lesion size $\geq$ 8 mm ($p < 0.001$), location in the same quadrant as the primary cancer ($p = 0.005$), delayed plateau kinetics ($p = 0.010$), T2 isointense ($p = 0.034$) and hypointense ($p = 0.024$) signals, and irregular mass shape ($p = 0.028$) were associated with malignancy. In comparison with the BI-RADS category, the scoring system based on these features with suspicious non-mass internal enhancement increased the diagnostic performance (area under the receiver operating characteristic curve: 0.918 vs. 0.727) and detected three false-negative cases. With this scoring system, 22 second-look ultrasound examinations (22/66, 33.3%) could have been avoided.

Conclusion The scoring system based on the lesion size, location relative to the primary cancer, delayed kinetic features, T2 signal intensity, mass shape, and non-mass internal enhancement can provide a more accurate approach to evaluate MRI-detected lesions in breast cancer patients.

Index terms Breast; Magnetic Resonance Imaging; Ultrasonography; Neoplasms

INTRODUCTION

MRI is the most sensitive imaging tool for detecting breast cancer, with about 90% sensitivity (1, 2). Therefore, MRI is widely used as a screening tool for breast cancer in high-risk patients or for evaluating disease extent or multiplicity in known breast cancer patients. In evaluation of breast lesions on MRI, radiologists consider various features including morphologic and kinetic features in routine clinical practice. However, there is no highly specific imaging factor for discriminating malignancy from benign tumor. Which feature should be considered preferentially for determining whether a lesion is cancerous varies from case to case; thus, the specificity of MRI is less satisfactory, ranging from 40% to 80% (1-3). Moreover, assessment of ultrasonography (US)-occult or mammography-occult MRI-detected lesion can be more difficult due to their relatively small size, compared to the lesion found on US or mammography (4). Therefore, subsequent second-look US examinations or MRI-guided biopsy should be considered for many cases of a little bit suspicious MRI-detected lesions.

There have been many investigations regarding important clinical factors or suspicious imaging features of MRI-detected lesions (5-13). Both Demartini et al. (7) and Gutierrez et al. (8) emphasized clinical indication of preoperative MRI evaluation in breast cancer patients and patients 50 years of age or older in predicting malignancy of MRI-detected lesions. Many other researchers suggested that large lesion size, lesion type-mass, and delayed washout kinetics are common features indicative of malignancy (6-13). However, few studies have been conducted to determine suspicious radiologic features of MRI-detected lesions limited to preoperative MRI evaluation of breast cancer patients or to suggest the systematic scoring system to predict probability of malignancy.

Therefore, the present study aimed to identify MR imaging features predictive of malignancy for evaluating MRI-detected lesions in breast cancer patients and to design the scoring system to predict malignancy.

MATERIALS AND METHODS

PATIENTS AND LESIONS

This retrospective study was approved by the Institutional Review Board (IRB No. 2018-03-039). Informed consent was waived. Between January 2014 and August 2017, 505 patients performed preoperative breast MRI after a diagnosis of breast cancer. Out of 505 patients, 87 patients had MRI-detected breast lesions (initial US- and mammography-occult) with Breast Imaging-Reporting and Data System (BI-RADS) category 3 or higher in addition to the proven malignancy and were recommended for second-look US evaluation. Of the 87 patients, 19 were excluded because their final pathologic results of MRI-detected lesions were not confirmed or follow-up imaging evaluations were not conducted. Finally, 68 patients (mean age 52 years, range 38–73, all women) with 86 additionally MRI-detected lesions (mean size 11 mm, range 3–75) were included in this study. The characteristics of patients and lesions are summarized in Table 1.

MRI EVALUATION

All examinations were performed using the 3.0-T MR system (Signa HDxt; General Electric Medical Systems, Milwaukee, WI, USA) with a dedicated breast coil. Imaging sequences included axial and sagittal T2-weighted fat-suppressed fast spin echo images [repetition time/echo time (TR/TE) 5932/86 ms, field of view (FOV) 320 × 320 mm, slice thickness 3 mm, matrix size 384 × 256] and dynamic axial or sagittal T1-weighted 3D fast spoiled gradient recalled series (TR/TE 5.3/2.3, flip angle 10°, FOV 340 × 340 mm, slice thickness 1.6 mm, matrix size 320 × 288) with 1 pre-contrast set and 4 post-contrast sets at 1-, 2-, 3-, and 6-min after contrast injection. Gadoterate meglumine (Prohance; Guerbet, Auulnay-Sous-Bois, France) was injected into an antecubital vein using an automated injector (Spectris MR; Medrad Europe, Maastricht, the Netherlands) at a dose of 0.1 mmoL/kg of body weight and a rate of 3 mL/s, followed by a 20 mL saline flush.

One of 4 radiologists with 3- to 16-years of breast imaging experience originally interpreted MRI examinations right after the MRI scan and one radiologist (A.Y.P.) with 5-years of breast imaging retrospectively reviewed all examinations. If there was any discrepancy between the original report and the retrospective review, all breast radiologists discussed the MRI findings and achieved consensus. The following MRI features of MRI-detected lesions were interpreted: lesion size, lesion location relative to main cancer (contralateral, different quadrant or same quadrant), T2 signal intensity relative to adjacent normal parenchyma (hyperintense, isointense, or hypointense), kinetic feature on delayed phase [persistent, plateau, or washout on kinetic curve analysis for using the dedicated workstation (Functool, General Electric Medical Systems)] and other MRI features according to the 5th BI-RADS (MRI) lexicon (14).

DATA COLLECTIONS

The following clinical, radiologic, and histopathologic data were retrospectively collected: patient age, TNM stage of primary cancer, multiplicity and bilaterality of cancer, presence or absence of second-look US examination, lesion detectability of MRI-detected lesions on second-look US, and histopathologic results of primary cancer (*in situ* cancer vs. invasive cancer) and MRI-detected lesions.

Of the total 86 MRI-detected lesions, second-look US examinations were performed for 66

Table 1. Patient and Lesion Characteristics

|	
Number of patients	*n* = 68
Mean age, range	52 years, 38–73
Number of lesions	*n* = 86
Number of lesions per patient (%)	
1 lesion	53 (80.0)
2 lesions	12 (17.6)
3 lesions	3 (4.4)
Lesion size, range	11 mm, 3–75
Histopathologic results (%)	
Malignant	22 (25.6)
Benign	64 (74.4)

lesions (76.7%), and 51 lesions (77.3%, 51/66) were detected. For 56 MRI-detected lesions, percutaneous biopsy ($n = 14$) or surgical excision ($n = 44$) was performed, and the final histopathologic results were regarded as the standard reference of this study (benign group vs. malignant group). For the other 30 MRI-detected lesions, imaging follow-up was performed using US or MRI (mean follow-up period 942.8 days, range 257–1526 days). All lesions were stable in size ($n = 8$) or disappeared ($n = 22$) during the follow-up period and so were classified into the benign group. Seventeen lesions (33.3%) out of 51 lesions detected on second-look US were malignant, and 2 (13.3%) out of 15 lesions not detected on second-look US were malignant. Fig. 1 shows the flowchart of the diagnostic process for the 86 MRI-detected lesions.

STATISTICAL ANALYSIS

The sizes of primary cancer and the MRI-detected lesion as well as patient age were compared between the benign and malignant groups using Student's t-test. The optimal cut-off value of MRI-detected lesion size predicting malignancy was analyzed using receiver operating characteristic (ROC) curve analysis with the use of Youden's index (the highest sum of sensitivity and specificity). The associations between clinicoradiologic features of MRI-detected lesions and histopathologic results (benign versus malignant) were evaluated using Fisher's exact test and logistic regression analysis.

The scoring system was designed according to estimated malignant predictability (odds ratio, OR), based on the results from logistic regression analysis. Among MRI features with p values less than 0.05 in logistic regression analysis, those with OR < 5 were counted as point 0, those with OR $\geq$ 5 or < 10 were counted as point 1, and those with OR $\geq$ 10 were counted as point 2. The sum of each point was calculated as the score of lesion. The optimal cut-off value of the scoring system to predict malignancy was determined using ROC curve analysis at

Fig. 1. Flowchart of the diagnostic process for 86 MRI-detected lesions.
US = ultrasonography
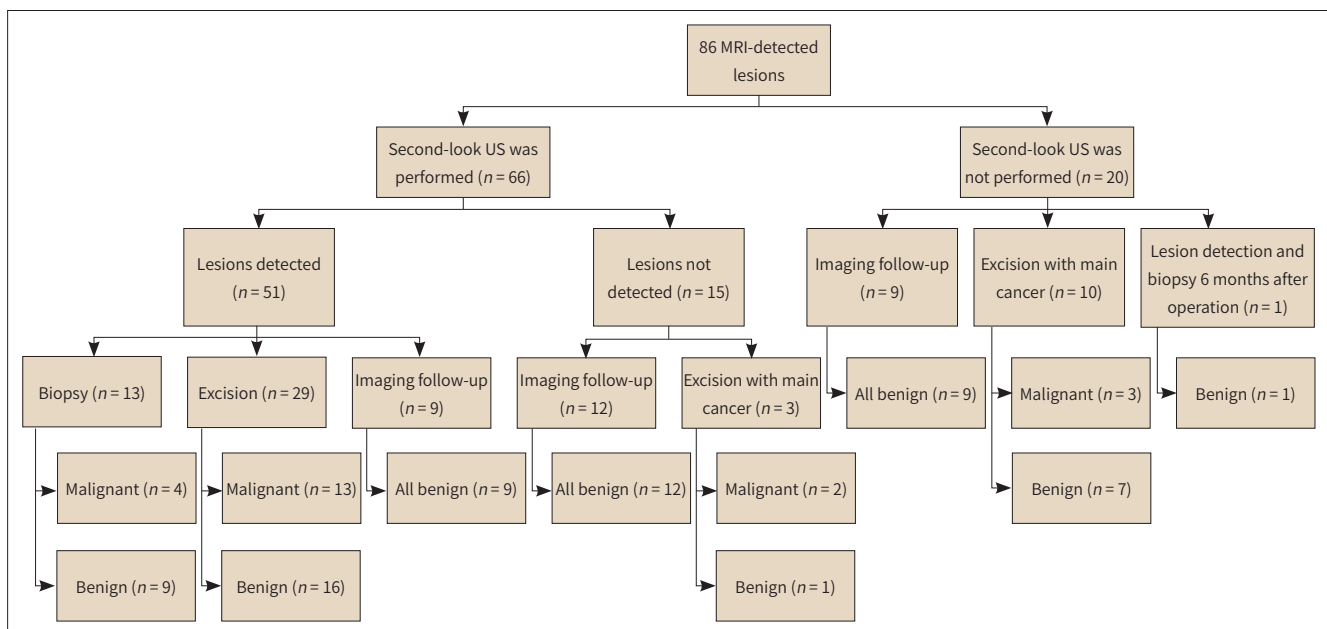
the level of 100% sensitivity and the highest specificity. The diagnostic performance of the scoring system was compared with that of BI-RADS category using McNemar test, relative predictive values, and the pairwise comparison of ROC curve by DeLong's test. Finally, the reduction rate of unnecessary second-look US examinations with the use of this model was calculated.

Statistical analyses were performed using SPSS for Window (version 23, IBM Corp., Armonk, NY, USA) and R (version 3.5.1, R foundation for Statistical Computing, Vienna, Austria). p values less than 0.05 were considered to be statistically significant.

RESULTS

HISTOPATHOLOGIC RESULTS

Of the 86 MRI-detected lesions, 64 (74.4%) were benign and 22 (25.6%) were malignant. The histologic types of the benign group included stromal fibrosis (n = 6), fibrocystic change (n = 4), sclerosing adenosis (n = 4), intraductal papilloma (n = 4), fibroadenomatous hyperplasia (n = 3), usual ductal hyperplasia (n = 2), intramammary lymph node (n = 2), fibroadenoma (n = 1), fat necrosis (n = 1), and unknown lesions that disappeared or were stable in size on follow-up imaging or that were removed via mastectomy but not additionally mentioned as concurrent cancer (n = 37). The histologic types of the malignant group included invasive ductal carcinoma (n = 10), ductal carcinoma *in situ* (n = 8), invasive lobular carcinoma (n = 2), intraductal papillary carcinoma (n = 1), and mucinous carcinoma (n = 1).

CLINICAL AND MRI FEATURES ASSOCIATED WITH MALIGNANCY

The sizes of MRI-detected lesions in the malignant group were larger than those in the benign group, but there was no significant statistical difference by Student's t-test (13.2 ± 14.4 mm vs. 9.6 ± 8.9 mm, p = 0.170). ROC curve analysis identified the optimal cut-off value of MRI-detected lesion size predicting malignancy as 8 mm with 86.4% sensitivity and 57.8% specificity. An MRI-detected lesion size of 8 mm or larger was significantly associated with malignancy (p < 0.001) (Table 2). Primary cancer size and patient age were not significantly different between the benign and malignant groups (primary cancer size, 24.3 ± 14.4 mm vs. 21.9 ± 8.6 mm, p = 0.367; patient age, 50.1 ± 7.4 years vs. 55.2 ± 10.2 years, p = 0.080).

MRI features associated with malignancy in MRI-detected lesions are summarized in Table 2. Kinetic features on delayed phase and BI-RADS category were significantly different between benign and malignant lesions (p = 0.019 and p < 0.001, respectively). Location relative to main cancer, Lesion type, mass shape, non-mass internal enhancement, and T2 signal intensity also appeared to be different between benign and malignant lesions with p-value of approximately 0.1 (p = 0.094, p = 0.081, p = 0.102, p = 0.115, and p = 0.102, respectively). In univariate logistic regression analysis, MRI-detected lesion size of 8 mm or larger, irregular mass shape rather than oval shape, plateau kinetics on delayed phase rather than persistent kinetics, and hypointensity on T2-weighted image rather than hyperintensity were associated with malignancy (p = 0.001, OR = 8.7; p = 0.041, OR = 3.9; p = 0.009, OR = 4.6; p = 0.042, OR = 5.2, respectively). The following clinicopathologic data and MRI features were not different between the benign and malignant groups: age with a cut-off value of 50 years (p = 0.621), T stage of main cancer (p = 0.587), N stage of main cancer (p = 0.774), multiplicity (p = 0.383), bilaterality (p =

Table 2. MRI Features Associated with Malignancy of Breast Lesions

MRI Features	Benign (n = 64, %)	Malignant* (n = 22, %)	p-Value[†]	Odds Ratio (95% CI)[‡]	p-Value[‡]
Lesion size, mm					
< 8	37 (92.8)	3 (13.6)	< 0.001	1	
≥ 8	27 (58.7)	19 (41.3)		8.7 (2.3–32.3)	0.001
Location relative to main cancer					
Contralateral	15 (83.3)	3 (16.7)	0.094	1	
Different quadrant	28 (82.4)	6 (17.6)		1.1 (0.2–4.9)	0.929
Same quadrant	21 (61.8)	13 (38.2)		3.1 (0.7–12.8)	0.119
Lesion type					
Mass	32 (66.7)	16 (33.3)	0.081	1	
Focus	16 (94.1)	1 (5.9)		0.1 (0.0–1.0)	0.053
Non-mass	16 (76.2)	5 (23.8)		0.6 (0.2–2.0)	0.431
Mass shape					
Oval	21 (77.8)	6 (22.2)	0.102	1	
Round	3 (75.0)	1 (25.0)		1.2 (0.1–13.4)	0.901
Irregular	8 (47.1)	9 (52.9)		3.9 (1.1–14.7)	0.041
Mass margin					
Circumscribed	18 (69.2)	8 (30.8)	0.651	1	
Irregular	11 (68.8)	5 (31.3)		1.0 (0.3–4.0)	0.974
Spiculated	3 (50.0)	3 (50.0)		2.3 (0.4–13.7)	0.378
Mass internal enhancement					
Homogeneous	21 (70.0)	9 (30.0)	0.172	1	
Heterogeneous	9 (75.0)	3 (25.0)		0.8 (0.2–3.6)	0.746
Rim	2 (33.3)	4 (66.7)		4.7 (0.7–30.2)	0.106
Non-mass distribution					
Focal	10 (83.3)	2 (16.7)	0.268	1	
Linear	0 (0)	1 (100)		N/A	N/A
Segmental	5 (71.4)	2 (28.6)		2.0 (0.2–18.7)	0.543
Regional	1 (100)	0 (0)		N/A	N/A
Non-mass internal enhancement					
Homogeneous	1 (100)	0 (0)	0.115		
Heterogeneous	13 (86.7)	2 (13.3)		N/A	N/A
Clumped	2 (50.0)	2 (50.0)		N/A	N/A
Clustered ring	0 (0)	1 (100)		N/A	N/A
Kinetics-delayed phase					
Persistent	42 (85.7)	7 (14.3)	0.019	1	
Plateau	13 (56.5)	10 (43.5)		4.6 (1.5–14.6)	0.009
Washout	9 (64.3)	5 (35.7)		3.3 (0.9–12.9)	0.082
T2 signal intensity					
Hyperintense	25 (86.2)	4 (13.8)	0.1020	1	
Isointense	33 (71.7)	13 (28.3)		2.5 (0.7–8.5)	0.153
Hypointense	6 (54.5)	5 (45.5)		5.2 (1.1–25.5)	0.042
Category on MRI					
3	39 (92.9)	3 (7.1)	< 0.001	1	
4	25 (62.5)	15 (37.5)		7.8 (2.0–29.7)	0.003
5	0 (0)	4 (100)		N/A	N/A

*Represents both malignant and high-risk lesions which need surgical excision.
[†]The results of Fisher's exact test.
[‡]The results of logistic regression analysis.
CI = confidence interval, N/A = not applicable

1.0), histopathologic result of main cancer ($p = 0.575$), amount of fibroglandular tissue ($p = 0.119$), level of background parenchymal enhancement ($p = 0.652$), margin of mass ($p = 0.651$), internal enhancement of mass ($p = 0.172$), and distribution of non-mass enhancement ($p = 0.268$).

MULTIVARIATE LOGISTIC REGRESSION ANALYSIS FOR PREDICTION OF MALIGNANCY

Multivariate logistic regression analyses for prediction of malignancy were performed for total lesions ($n = 86$) and for mass lesions ($n = 48$). For total lesions, MRI-detected lesion size of 8 mm or larger, the same quadrant location relative to the primary cancer rather than contralateral or ipsilateral different quadrant location, plateau kinetics on delayed phase rather than persistent kinetics, and iso- or hypointensity on T2-weighted image rather than hyperintensity were independent predictors of malignancy ($p < 0.001$, $p = 0.005$, $p = 0.010$, $p = 0.034$, and $p = 0.024$, respectively) (Table 3, Figs. 2, 3). Lesion type was not a significant feature predictive of malignancy in multivariate logistic regression analysis ($p = 0.997$ for focus vs. mass, $p = 0.467$ for non-mass enhancement vs mass). For mass lesions, MRI-detected lesion size of 8 mm or larger, the same quadrant location relative to the primary cancer rather than contralateral or ipsilateral different quadrant location, irregular mass shape rather than oval or round shape, and plateau kinetics on delayed phase rather than persistent kinetics were independent predictors of malignancy ($p = 0.012$, $p = 0.038$, $p = 0.028$, and $p = 0.038$, respectively) (Table 3). For non-mass enhancement or focus lesion, multivariate logistic regression analysis

Table 3. Multivariate Logistic Regression Analysis to Predict Malignancy

Total Lesions ($n = 86$)			Mass Lesions ($n = 48$)		
MRI Features	Odds Ratio (95% CI)	*p*-Value	MRI Features	Odds Ratio (95% CI)	*p*-Value
Lesion size, mm			Lesion size, mm		
< 8	1		< 8	1	
≥ 8	30.4 (4.6–199.6)	< 0.001	≥ 8	538.9 (4.0–7319.7)	0.012
Location relative to main cancer			Location relative to main cancer		
Contralateral	1		Contralateral	1	
Different quadrant	2.2 (0.3–18.0)	0.452	Different quadrant	2.4 (0.1–111.4)	0.663
Same quadrant	22.0 (2.6–188.3)	0.005	Same quadrant	265.1 (1.3–52298.2)	0.038
Lesion type			Mass shape		
Mass	1		Oval	1	
Focus	1 (0.1–17.7)	0.997	Round	10.0 (0.1–1561.6)	0.371
Non-mass	0.5 (0.1–3.1)	0.467	Irregular	75.3 (1.6–3592.2)	0.028
Kinetics-delayed phase			Kinetics-delayed phase		
Persistent	1		Persistent	1	
Plateau	8.2 (1.6–41.3)	0.010	Plateau	207.3 (1.3–31948.0)	0.038
Washout	5.4 (0.9–34.1)	0.071	Washout	9.0 (0.1–976.5)	0.359
T2 signal intensity			T2 signal intensity		
Hyperintense	1		Hyperintense	1	
Isointense	6.6 (1.2–37.5)	0.034	Isointense	13.1 (0.5–358.5)	0.480
Hypointense	18.0 (1.5–219.6)	0.024	Hypointense	54.8 (0.3–9535.0)	0.128

CI = confidence interval

Fig. 2. A 47-year-old woman with invasive ductal carcinoma.
A. Gray-scale ultrasonography (left) and early dynamic contrast-enhanced subtraction MRI (right) show a 13-mm mass, confirmed as invasive ductal carcinoma on biopsy, in the lower outer quadrant of the left breast (arrows).
B. Axial early (upper left) and delayed (upper right) dynamic contrast-enhanced subtraction MRI, kinetic curve (lower left), and axial T2-weighted fat-suppressed image (lower right) show another 8-mm oval circumscribed mass with early fast and delayed plateau enhancement and T2 isointense signal in the same quadrant as the primary cancer, assessed as category 4 with a score of 7 (arrows).
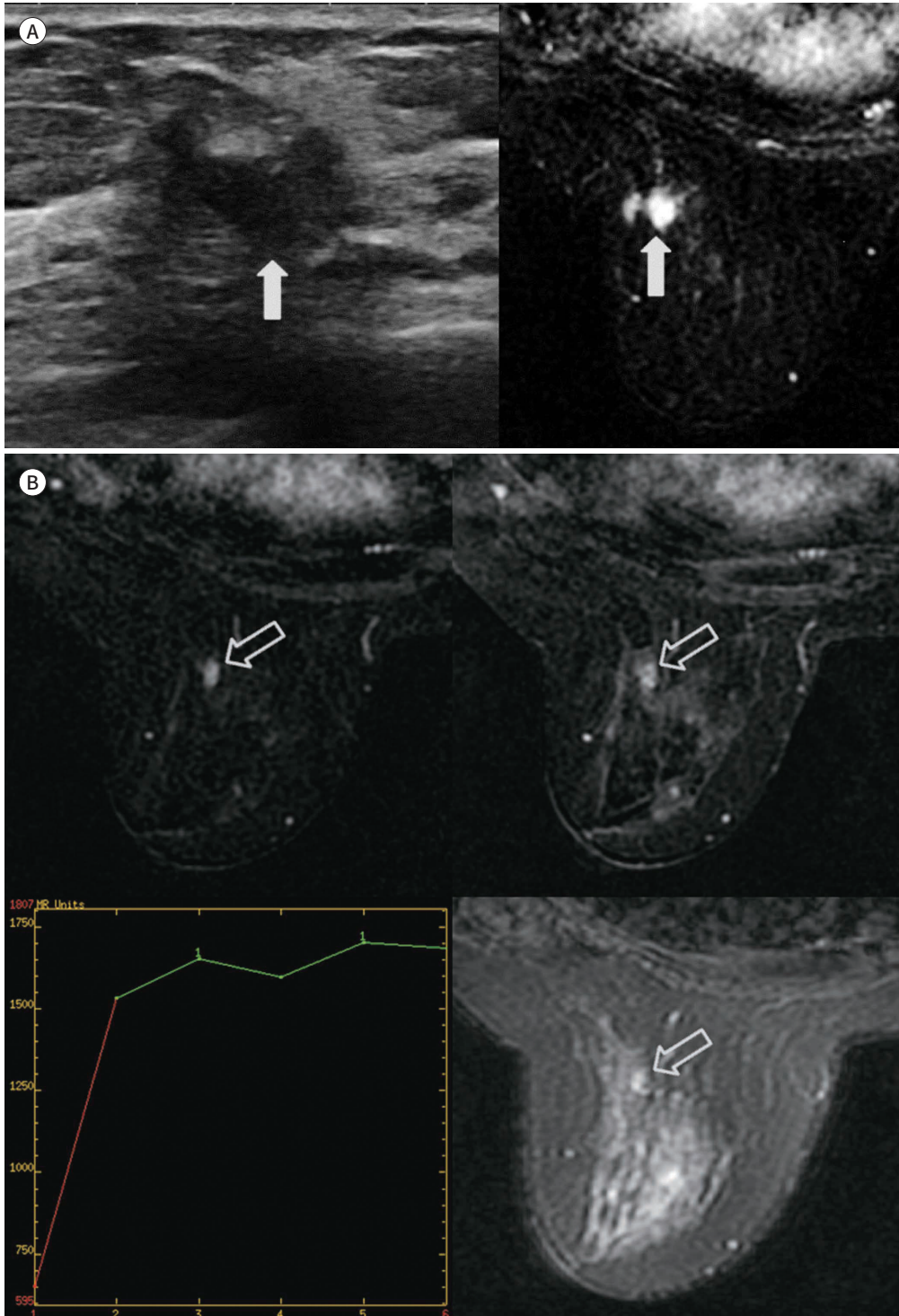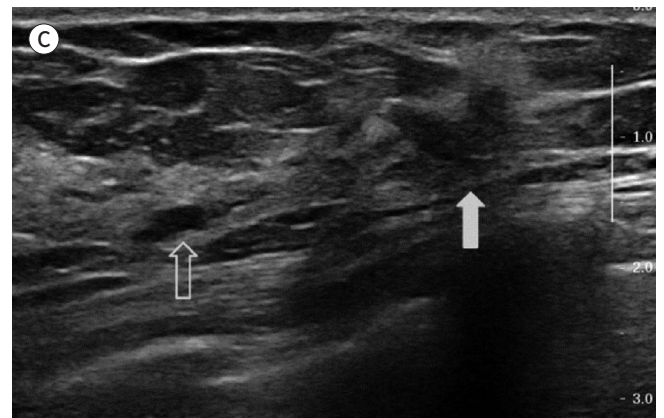
Fig. 2. A 47-year-old woman with invasive ductal carcinoma.
C. Second-look US correlates with MRI-detected lesion (open arrow), 1 cm from the primary cancer (arrow), assessed as category 4B. US-guided wire localization and excision for the MRI-detected lesion revealed ductal carcinoma *in situ*.
US = ultrasonography

could not be performed due to a small number of lesions.

THE SCORING SYSTEM TO PREDICT PROBABILITY OF MALIGNANCY

To design the scoring system, the 5 above-mentioned independent predictors of malignancy (MRI-detected lesion size, lesion location relative to main cancer, kinetic features on delayed phase, T2 signal intensity, and mass shape) and non-mass internal enhancement were included. Non-mass internal enhancement was included in the scoring system in spite of relatively low statistical evidence (p = 0.115 in Fisher's exact test), because the most significant morphologic feature for non-mass enhancement, corresponding to mass shape was necessary to increase the explanatory power of the scoring system, not only for mass lesions but also for non-mass enhancement lesions. Clumped enhancement and clustered ring non-mass enhancement seem to be associated with malignancy, although an OR could not be calculated due to the small number of non-mass enhancement lesions (Table 2). Table 4 summarizes the scoring system to predict probability of malignancy according to estimated malignant predictability.

The mean score of malignant lesions was significantly higher than that of benign lesions (6.6 ± 1.2 vs. 3.8 ± 1.5, p < 0.001). The area under the ROC curve (AUC) of the scoring system was 0.918. The optimal cut-off value of the scoring system to predict malignancy was score 5 or higher and its diagnostic performance was 100% sensitivity, 65.6% specificity, 50% positive predictive value (PPV), 100% negative predictive value (NPV), 74.4% accuracy, and 0.828 AUC. When BI-RADS category 3 lesions are assigned as benign and 4 or 5 lesions as malignant, the diagnostic performance of BI-RADS category was relatively low in sensitivity (86.4%), NPV (92.9%), accuracy (67.4%), and AUC (0.737) in comparison with that of the scoring system. Table 5 summarizes the comparison of diagnostic performance between scoring system and BI-RADS category.

If we apply the scoring system to this study population, only 44 lesions required second-look US examination without false-negative cases, and unnecessary second-look US examinations could have been avoided for 22 lesions (the reduction rate 33.3%, 22/66). When we consider that second-look US examinations are performed only for MRI-detected lesions with BI-RADS category 4 or 5 on MRI (n = 44), 3 malignant lesions can be missed. The scoring system can eliminate these 3 false-negative cases, although there is no additional reduction of unnecessary second-look US examinations.

Fig. 3. A 48-year-old woman with invasive ductal carcinoma.
A. Gray-scale ultrasonography (left) and early dynamic contrast-enhanced subtraction MRI (right) show a 30-mm mass, confirmed as invasive ductal carcinoma on biopsy, in the lower medial quadrant of the left breast (arrows).
B. Sagittal early (upper left) and delayed (upper right) dynamic contrast-enhanced subtraction MRI, kinetic curve (lower left), and sagittal T2-weighted fat-suppressed image (lower right) show another 6-mm irregular mass with early fast and delayed persistent enhancement and T2 isointense signal in the upper medial quadrant of the left breast, assessed as category 4 with a score of 3 (arrows).
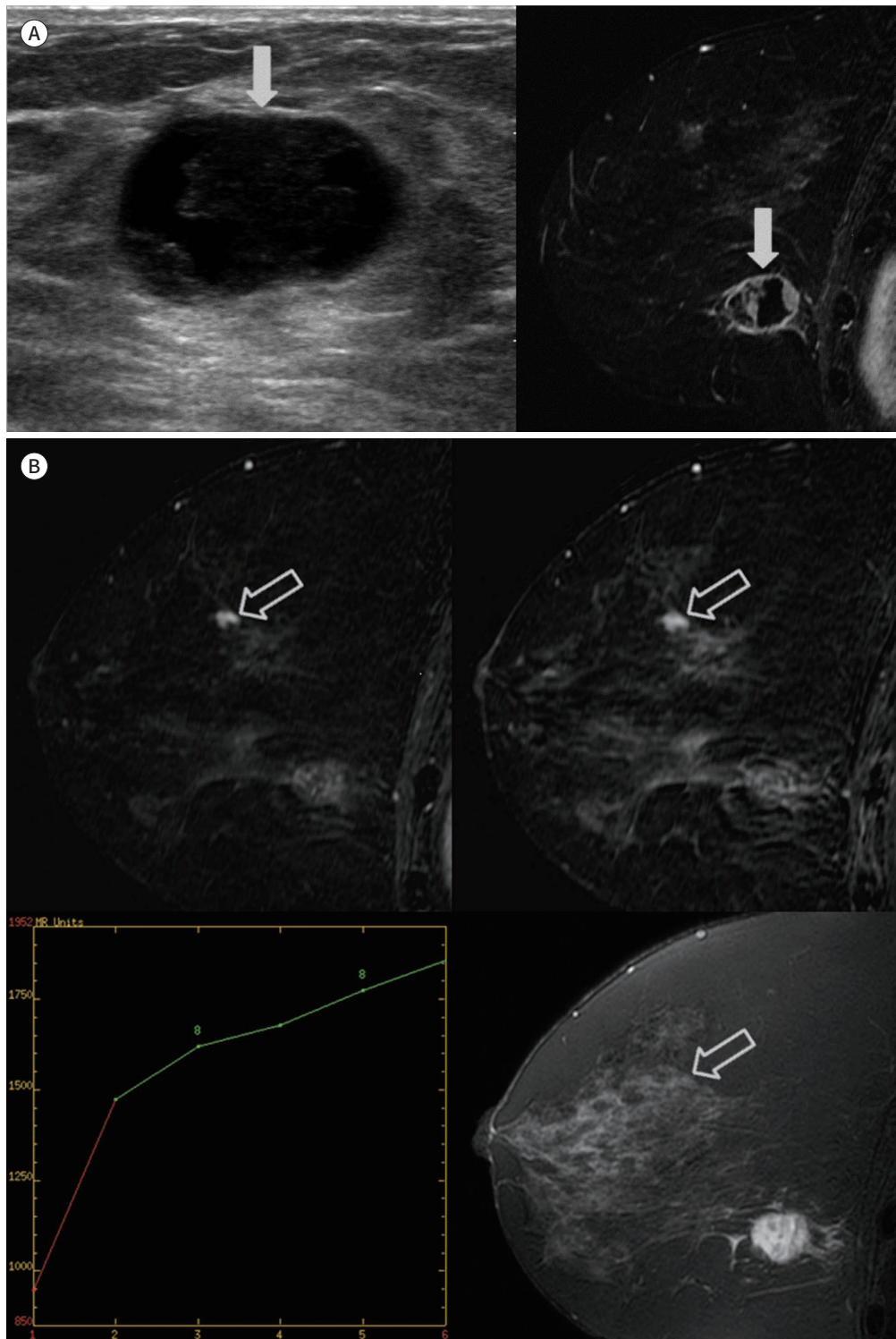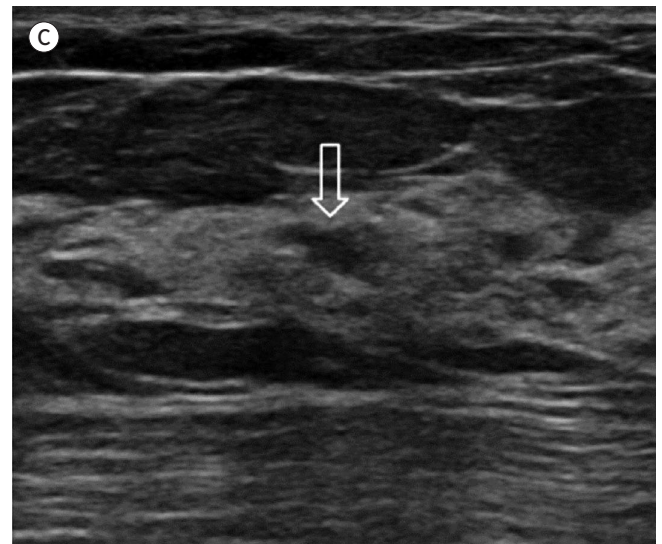
Fig. 3. A 48-year-old woman with invasive ductal carcinoma.
C. Second-look US correlates with MRI-detected lesion (arrow) at the 11 o'clock position in the left breast, assessed as category 4A. US-guided core needle biopsy revealed stromal fibrosis.
US = ultrasonography

Table 4. Scoring System Based on the Estimated Malignant Predictability

MRI Features	0	1	2
Lesion size, mm	< 8		≥ 8
T2 signal intensity	Hyperintense	Isointense	Hypointense
Location relative to main cancer	Contralateral or different quadrant		Same quadrant
Kinetics-delayed phase	Persistent		Plateau or washout
Mass shape	Oval or round	Irregular	
Non-mass internal enhancement	Homogeneous or heterogeneous	Clumped or clustered ring	

Table 5. Comparison of Diagnostic Performance between the Scoring System and the BI-RADS Category

	Sensitivity	Specificity	PPV	NPV	Accuracy	AUC
Scoring system*	100	65.6	50	100	74.4	0.918
BI-RADS category[†]	86.4	60.9	43.2	92.9	67.4	0.737
p-value	0.083	0.491	0.187	0.083	N/A	< 0.001

*Scoring system according to estimated malignant predictability with the optimal cut-off score 5.
[†]BI-RADS category 4 or 5 was regarded as the prediction of malignancy.
AUC = area under the receiver operating characteristic curve, BI-RADS = Breast Imaging-Reporting and Data System, NPV = negative predictive value, PPV = positive predictive value

DISCUSSION

In the present study, lesion size, location relative to primary cancer, T2 signal intensity, delayed kinetic feature, and irregular mass shape were important imaging features for evaluating MRI-detected lesions on preoperative breast MRI of breast cancer patients.

Lesion size of 8 mm or larger was the most predictive feature predicting malignancy in this study. Many preceding studies also stressed that large lesion size is an important feature suggesting malignancy, although the size criteria vary among studies (7, 9, 11, 13). Both Demartini et al. (7) and Gutierrez et al. (13) stated that a lesion size of 10 mm or greater suggests increased likelihood of malignancy. Linda et al. (11) asserted that three different size criteria (≥ 6, 11,

and 16 mm) are all associated with malignancy. Liberman et al. (9) suggested that the frequency of malignancy significantly increased with increasing lesion size (p = 0.0005), and that most lesions smaller than 5 mm are benign (3% of likelihood of malignancy). The size criterion of 8 mm in this study is slightly lower than that of other studies (10 mm is common), which may result from using a different study population. The present study only targeted preoperative MRI cases in breast cancer patients, while previous studies included MRI examinations with various indications such as screening or follow-up. In assessment of MRI-detected lesions on preoperative MRI for known breast cancer, a tighter size standard might be required.

The location of MRI-detected lesion relative to the primary cancer was another significant factor associated with malignant potential. The MRI-detected lesions located in the same quadrant as the primary cancer were more frequently malignant compared with those located in the contralateral breast or in a different quadrant of the ipsilateral breast. This result is supported by previous investigations (15-19). The prevalence of ipsilateral multifocal or multicentric cancers ranges from 14% to 47% (15, 16), while that of synchronous bilateral cancer ranges from 1% to 3% (17, 18). Liberman et al. (19) reported that preoperative MRI detected mammography- or US-occult ipsilateral additional cancer in 19 of 70 breast cancer patients (27%), and the additional cancer was located in the same quadrant as the main cancer in 14 of 19 patients. Therefore, radiologists should more carefully analyze MRI-detected lesions located in the same quadrant as the primary cancer.

In the present study, T2 hypointensity or isointensity of MRI-detected lesion was a predictive sign of malignancy. This result is similar to those of preceding studies (20, 21). For example, Kuhl et al. (20) reported that 87% of cancers showed iso- or hypointensity with respect to normal parenchyma, while Arponen et al. (21) reported that low T2 signal intensity yielded high specificity (80%) in diagnosing malignancy. These results are caused by the histopathological features of breast cancers including abundant cellularity, perilesional fibrosis, and a high nucleus-to-plasma ratio (20). Although the utility of T2-weighted image in discriminating breast cancer from benign tumors is still controversial (22, 23), the current study suggests that T2 hypo- or iso-intensity of MRI-detected lesions can be an additional useful finding in predicting malignancy.

The kinetic feature in dynamic contrast-enhanced MRI study is the most widely discussed parameter in evaluating breast lesions. Most studies report that the delayed washout kinetic feature is associated with malignancy (6, 10, 12, 24, 25). Rapid contrast enhancement washout of breast cancer is explained by high tissue vascularity, vessel permeability, and diffusion in the extra-vascular space (10). In evaluating MRI-detected breast lesions, Demartini et al. (7) stated that washout kinetics showed the strongest association with malignancy compared with persistent kinetics (OR 4.2). In this study, the delayed kinetic features were significantly different between benign and malignant tumors, but in multivariate analysis, plateau kinetics was more associated with malignancy compared with washout kinetics. This result might be due to a relatively small lesion population and small lesion size. Because tumor angiogenesis is directly associated with tumor growth, the small cancers identified in this study may present less a suspicious plateau kinetic feature rather than a washout feature (26).

Most significant morphologic descriptors were shape for mass and internal enhancement characteristics for non-mass enhancement. According to previous studies, suspicious MRI

features with the highest PPV in mammography-occult, MRI-detected mass lesions included irregular or spiculated margin as well as irregular shape (5, 23). However, the current study resulted that only an irregular shape is the statistically significant feature predicting malignancy. We guess that the size of mass lesions in this study is small (mean size 7.9 mm, range 5–13 mm) and thus there could be a considerable overlap in interpretation of margin between benign and malignant lesions. For non-mass enhancement lesions, meanwhile, internal enhancement characteristics showed less significant statistical difference between benign and malignant lesions ($p = 0.115$) probably due to small study population, but clumped (50% malignancy) and clustered ring (100% malignancy) enhancement seem to associated with malignancy, not differently from preceding reports (5, 27).

The scoring system based on lesion size, location relative to main cancer, delayed kinetic features, T2 signal intensity, mass shape and non-mass internal enhancement showed higher AUC in comparison with BI-RADS category. And with the cut-off score 5 or more, the scoring system provided 100% sensitivity (no false-negative case) without additional requirements of second-look US examinations. Furthermore, among 66 patients performing second-look US examinations in this study, 22 patients could have avoided unnecessary second-look US examinations with this scoring system, although some lesions with BI-RADS category 3 on MRI were included in this study. However, 3 lesions assessed as BI-RADS category 3 were malignant and the application of scoring system can eliminate these 3 false-negative cases. Therefore, this scoring system could be helpful in predicting malignancy for MRI-detected lesions in breast cancer patients and deciding the necessity of additional US examinations more accurately in comparison with subjective category assessment.

Our study has several limitations. First, this study included a relatively small population, and the explanatory power of the scoring system for prediction of malignancy should be validated in larger population set. Second, computer-aided diagnosis (CAD) for kinetic curve analysis was not applied in this study. With references to several preceding studies, use of a CAD system for the whole lesion evaluation can provide more objective information in evaluation of MRI-detected lesions (12, 28, 29). A large-scale investigation with more accurate evaluation using CAD system should be performed in the future.

In conclusion, in evaluation of additional MRI-detected lesion on preoperative MRI of breast cancer patients, the scoring system based on lesion size, location relative to main cancer, delayed kinetic feature, T2 signal intensity, mass shape and non-mass internal enhancement could be helpful to predict malignancy and to reduce unnecessary second-look US examinations.

Author Contributions

Conflicts of Interest

The authors have no potential conflicts of interest to disclose.

REFERENCES

1. Bluemke DA, Gatsonis CA, Chen MH, DeAngelis GA, DeBruhl N, Harms S, et al. Magnetic resonance imaging

of the breast prior to biopsy. *JAMA* 2004;292:2735-2742

2. Lehman CD, Gatsonis C, Kuhl CK, Hendrick RE, Pisano ED, Hanna L, et al. MRI evaluation of the contralateral breast in women with recently diagnosed breast cancer. *N Engl J Med* 2007;356:1295-1303

3. Orel SG, Schnall MD. MR imaging of the breast for the detection, diagnosis, and staging of breast cancer. *Radiology* 2001;220:13-30

4. Meissnitzer M, Dershaw DD, Lee CH, Morris EA. Targeted ultrasound of the breast in women with abnormal MRI findings for whom biopsy has been recommended. *AJR Am J Roentgenol* 2009;193:1025-1029

5. Mahoney MC, Gatsonis C, Hanna L, DeMartini WB, Lehman C. Positive predictive value of BI-RADS MR imaging. *Radiology* 2012;264:51-58

6. Pinker-Domenig K, Bogner W, Gruber S, Bickel H, Duffy S, Schernthaner M, et al. High resolution MRI of the breast at 3 T: which BI-RADS® descriptors are most strongly associated with the diagnosis of breast cancer? *Eur Radiol* 2012;22:322-330

7. Demartini WB, Kurland BF, Gutierrez RL, Blackmore CC, Peacock S, Lehman CD. Probability of malignancy for lesions detected on breast MRI: a predictive model incorporating BI-RADS imaging features and patient characteristics. *Eur Radiol* 2011;21:1609-1617

8. Gutierrez RL, Demartini WB, Eby P, Kurland BF, Peacock S, Lehman CD. Clinical indication and patient age predict likelihood of malignancy in suspicious breast MRI lesions. *Acad Radiol* 2009;16:1281-1285

9. Liberman L, Mason G, Morris EA, Dershaw DD. Does size matter? Positive predictive value of MRI-detected breast lesions as a function of lesion size. *AJR Am J Roentgenol* 2006;186:426-430

10. Nogueira L, Brandão S, Matos E, Gouveia Nunes R, Ferreira HA, Loureiro J, et al. Improving malignancy prediction in breast lesions with the combination of apparent diffusion coefficient and dynamic contrast-enhanced kinetic descriptors. *Clin Radiol* 2015;70:1016-1025

11. Linda A, Zuiani C, Londero V, Bazzocchi M. Outcome of initially only magnetic resonance mammography-detected findings with and without correlate at second-look sonography: distribution according to patient history of breast cancer and lesion size. *Breast* 2008;17:51-57

12. Wang LC, DeMartini WB, Partridge SC, Peacock S, Lehman CD. MRI-detected suspicious breast lesions: predictive values of kinetic features measured by computer-aided evaluation. *AJR Am J Roentgenol* 2009;193:826-831

13. Gutierrez RL, DeMartini WB, Eby PR, Kurland BF, Peacock S, Lehman CD. BI-RADS lesion characteristics predict likelihood of malignancy in breast MRI for masses but not for nonmasslike enhancement. *AJR Am J Roentgenol* 2009;193:994-1000

14. Morris EA, Comstock CE, Lee CH, Lehman CD, Ikeda DM, Newstead GM, et al. *ACR BI-RADS Magnetic Resonance Imaging*. In American College of Radiology, ed. *ACR BI-RADS Atlas, Breast Imaging Reporting and Data System*. Reston, VA: American College of Radiology 2013

15. Lagios MD, Westdahl PR, Rose MR. The concept and implications of multicentricity in breast carcinoma. *Pathol Annu* 1981;16:83-102

16. Holland R, Veling SH, Mravunac M, Hendriks JH. Histologic multifocality of Tis, T1-2 breast carcinomas. Implications for clinical trials of breast-conserving surgery. *Cancer* 1985;56:979-990

17. Heron DE, Komarnicky LT, Hyslop T, Schwartz GF, Mansfield CM. Bilateral breast carcinoma: risk factors and outcomes for patients with synchronous and metachronous disease. *Cancer* 2000;88:2739-2750

18. Hungness ES, Safa M, Shaughnessy EA, Aron BS, Gazder PA, Hawkins HH, et al. Bilateral synchronous breast cancer: mode of detection and comparison of histologic features between the 2 breasts. *Surgery* 2000;128:702-707

19. Liberman L, Morris EA, Dershaw DD, Abramson AF, Tan LK. MR imaging of the ipsilateral breast in women with percutaneously proven breast cancer. *AJR Am J Roentgenol* 2003;180:901-910

20. Kuhl CK, Klaschik S, Mielcarek P, Gieseke J, Wardelmann E, Schild HH. Do T2-weighted pulse sequences help with the differential diagnosis of enhancing lesions in dynamic breast MRI? *J Magn Reson Imaging* 1999;9:187-196

21. Arponen O, Masarwah A, Sutela A, Taina M, Könönen M, Sironen R, et al. Incidentally detected enhancing lesions found in breast MRI: analysis of apparent diffusion coefficient and T2 signal intensity significantly improves specificity. *Eur Radiol* 2016;26:4361-4370

22. Yuen S, Uematsu T, Kasami M, Tanaka K, Kimura K, Sanuki J, et al. Breast carcinomas with strong high-signal intensity on T2-weighted MR images: pathological characteristics and differential diagnosis. *J Magn*

Reson Imaging 2007;25:502-510

23. Liberman L, Morris EA, Lee MJ, Kaplan JB, LaTrenta LR, Menell JH, et al. Breast lesions detected on MR imaging: features and positive predictive value. *AJR Am J Roentgenol* 2002;179:171-178

24. Fujiwara K, Yamada T, Kanemaki Y, Okamoto S, Kojima Y, Tsugawa K, et al. Grading system to categorize breast MRI in BI-RADS 5th edition: a multivariate study of breast mass descriptors in terms of probability of malignancy. *AJR Am J Roentgenol* 2018;210:W118-W127

25. Partridge SC, Rahbar H, Murthy R, Chai X, Kurland BF, DeMartini WB, et al. Improved diagnostic accuracy of breast MRI through combined apparent diffusion coefficients and dynamic contrast-enhanced kinetics. *Magn Reson Med* 2011;65:1759-1767

26. Folkman J. Angiogenesis and breast cancer. *J Clin Oncol* 1994;12:441-443

27. Uematsu T, Kasami M. High-spatial-resolution 3-T breast MRI of nonmasslike enhancement lesions: an analysis of their features as significant predictors of malignancy. *AJR Am J Roentgenol* 2012;198:1223-1230

28. Gweon HM, Cho N, Seo M, Chu AJ, Moon WK. Computer-aided evaluation as an adjunct to revised BI-RADS Atlas: improvement in positive predictive value at screening breast MRI. *Eur Radiol* 2014;24:1800-1807

29. Williams TC, DeMartini WB, Partridge SC, Peacock S, Lehman CD. Breast MR imaging: computer-aided evaluation program for discriminating benign from malignant lesions. *Radiology* 2007;244:94-103

유방암 환자의 MRI에서 발견된 병변의 악성 예측을 위한 점수체계: 진단적 능력과 이차 초음파 결정에 미치는 영향

권영걸 · 박아영*

목적 유방암 환자의 MRI에서 발견된 추가적 병변의 악성 예측을 위한 점수체계를 설계하고자 하였다.

대상과 방법 68명 유방암 환자의 86개 MRI 발견 병변(64 양성, 22 악성)이 후향적으로 연구되었다. 스튜던트 t 검정, Fisher 정확검정, 로짓 회귀분석을 이용해 영상적 소견과 조직학적 결과의 상관관계를 분석했다. 의미 있는 악성 시사 소견을 기반으로 한 점수체계를 설계하고 그것의 진단적 능력을 Breast Imaging-Reporting and Data System (이하 BI-RADS) category와 비교하였다.

결과 병변 크기 $\geq$ 8 mm ($p <$ 0.001), 주 병소와 동일한 사분면에 위치($p =$ 0.005), 지연기의 고원형 조영 증강($p =$ 0.010), T2 등신호($p =$ 0.034) 혹은 저신호 강도($p =$ 0.024), 불규칙한 종괴 모양($p =$ 0.028)이 악성과 관련 있었다. 이 소견들과 의심스러운 비종괴 내부 조영 양상을 바탕으로 한 점수체계는 BI-RADS의 진단적 능력을 향상시켰고(area under the curve, 0.918 vs. 0.727), 3개의 위음성 케이스를 방지할 수 있었다. 또한, 22개의 불필요한 2차 초음파 검사(22/66, 33.3%)를 줄일 수 있었다.

결론 병변 크기, 주 병소와의 상대적 위치, 지연기의 조영 증강 양상, T2 신호강도, 종괴의 모양 및 비종괴 내부 조영 양상을 기반으로 한 점수체계는 유방암 환자의 MRI 발견 병소를 평가하는데 있어 정확도를 높여 줄 수 있다.

차의과학대학교 분당차병원 영상의학과